**Journal of Electrical and Electronic Engineering**
2023; 11(3): 67-76
http://www.sciencepublishinggroup.com/j/jeee
doi: 10.11648/j.jeee.20231103.11
ISSN: 2329-1613 (Print); ISSN: 2329-1605 (Online)

# Low Electromagnetic Coupling Achievement of a Quad-Element UWB MIMO Antenna Using Miniaturization Technique

**Aicha Mchbal*, Naima Amar Touhami, Abdelhafid Marroun**

Physics Department, Abdelmalek Essaadi University, Tetuan, Morocco

**Email address:**
aicha.mchbal8@gmail.com (Aicha Mchbal)
*Corresponding author

**To cite this article:**
Aicha Mchbal, Naima Amar Touhami, Abdelhafid Marroun. Low Electromagnetic Coupling Achievement of a Quad-Element UWB MIMO Antenna Using Miniaturization Technique. *Journal of Electrical and Electronic Engineering*. Vol. 11, No. 3, 2023, pp. 67-76.
doi: 10.11648/j.jeee.20231103.11

**Received**: April 10, 2023; **Accepted**: May 9, 2023; **Published**: June 20, 2023

**Abstract:** This research presents a study of a four-element MIMO antenna, whose objective is to design a miniaturized or a reduced inter-elements spacing of a quad–element MIMO antenna that operates in UWB spectrum ranging between 3.1-10.6 GHz, and that characterizes by a reduced inter-element electromagnetic coupling which is due to nearfield coupling and surface current propagation between ports. The proposed MIMO antenna radiating elements are developed from a simple rectangular patch antenna. With the aim to reduce the electromagnetic coupling between radiators and cover the whole UWB bandwidth, diverse techniques are employed, including the employment of the polarization diversity technique, whereas the use of decoupling structures is prevented so as to avoid a bulky antenna assembly. Measurements show that the studied UWB MIMO antenna is characterized by a good compactness whose dimension is about 31×31×0.8 $mm^3$, and it offers a -10 dB impedance bandwidth of 3-12.8 GHz, a mutual coupling <-15 dB, correlation coefficients<0.3, a diversity gain of about 8.75 and a total active reflection coefficient less than -12 dB. Results prove that despite of the miniaturized size of the studied antenna assembly and the disuse of decoupling mechanisms, the presented antenna provides potential diversity performances for use in UWB applications.

**Keywords:** MIMO Assembly, Electromagnetic Coupling, Decoupling Mechanisms, Diversity Techniques, UWB Applications

## 1. Introduction

The rapid growth of miniaturized communications equipment that does not require a physical wire, has push researchers to design novel antennas that are characterized by a high performance. As a result, there is a high demand for compact, low profile UWB antennas qualified by their ability to perform well. Among the main purposes in recent radio systems, like UWB systems, is to take footprint size into consideration while building integrated circuits whose size must be small in order to meet portable wireless devices requirements. Therefore, antenna dimension is regarded as a priority in the design of UWB systems. Planar technology can be a good alternative in order to have a reduced volume of UWB antennas since it is based on the planar version of radiator, which makes realizing a prototype at the fabrication level simple and easy. Thus, the integration of the antenna of interest into RF circuits becomes feasible as exposed in paper [1].

The use of radio equipments knows a high in information technology, and there is a high demand for small footprint of radio electronic equipments, as well as an increase in the amount of data transmitted during a specified time for these equipments. According to this, UWB MIMO antenna systems are being known for their better performance as shown in article [2].

In general, the proportion of mutual coupling for each element in the MIMO array rely on various factors, including: distance between radiators, radiation pattern of each antenna element, assembly geometry, relative arrangement of the antenna element in the system, operating frequency, and near-field dispersions, see research [3]. Referring to the same reference, the implementation of MIMO technology on small personal communication devices requires multiple antennas to be arranged close to each other. Therefore, electromagnetic coupling affects the performance of MIMO communication. Many studies have investigated the impact of electromagnetic coupling on MIMO systems. In order to minimize this coupling phenomenon, various methods exist in the literature, we find:

Techniques to suppress antenna inter-element coupling through the shared ground plane: in this categorization, diverse perspectives are introduced, including: defective ground plane structures what is called (DGS), band gap structures (EBG), slot structures insertion, stub insertion (GND), current localization structures (CLS), or the pin/via shorting approach, as cited in paper [4]. Then there are techniques to suppress antenna inter-element coupling by space wave radiation: in this categorization various methods are exposed, including space between antenna radiating elements, decoupling wall structures (DWS), neutralization line (NL), decoupling and matching networks (DMN), parasitic structures, or outrightly the use of metamaterials (MTM), as mentioned in article [5]. And last but not least there are techniques for the suppression of antenna coupling by near field coupling: which is mainly based on the introduction of parasitic resonant slots for the suppression of near field coupling between closely spaced antennas, like used in research [6]. The overarching question that this work attempts to answer is how to design a compact and efficient multi-antenna system without using any of the mentioned decoupling techniques to provide a compact high-performance MIMO system.

## 2. The Design Process

### *2.1. Single Antenna*

Let's start now with the design of the single antenna. In fact, the design of this latter is based on a simple rectangular patch antenna (see Figure 1) with narrow bandwidth that has been transformed into a structure that meeting the bandwidth criteria. As we know, for a rectangular patch, the bandwidth generally depends on the geometry of the antenna, the relative permittivity of the substrate as well as its thickness h, see reference [7].

To highlight this, we considered a rectangular patch printed on a substrate of thickness h =0.8 mm. And for a resonance frequency of 6.85 GHz which obviously belongs to the UWB technology. The following analytical expressions that are extracted from paper [8] have been used in order to determine the proposed single antenna dimensions:

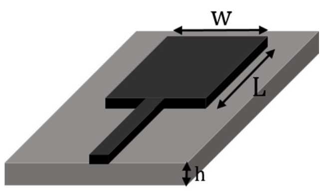


***Figure 1.*** *Simple rectangular patch antenna.*

$$L = \frac{c}{2f_r\sqrt{\mathcal{E}_{reff}}} - 2\Delta L \quad (1)$$

$$\Delta L = 0.412h\frac{(\mathcal{E}_{reff}+0.3)\left(\frac{W}{h}+0.264\right)}{(\mathcal{E}_{reff}-0.258)\left(\frac{W}{h}+0.8\right)} \quad (2)$$

$$\mathcal{E}_{reff} = \frac{\mathcal{E}_r+1}{2} + \frac{\mathcal{E}_r-1}{2}\left[1+12\frac{h}{W}\right]^{\frac{-1}{2}} \quad (3)$$

Where:
c: is the speed of light in air, f is the frequency.
L: is the resonant length of the patch.
W: is its width.
h et $\mathcal{E}_{reff}$: are the thickness of the substrate and its effective permittivity, respectively.

The width of the antenna is given by the following expression in article [9]:

$$W = \frac{\lambda_0}{2}\left(\frac{\mathcal{E}_r+1}{2}\right)^{-\frac{1}{2}} \quad (4)$$

Then, with the purpose of covering a wide bandwidth, a partial ground plane was used, with a defected ground structure which is a combination of three slots that take place the ground and whose objective is the impedance matching enhancement. Furthermore, with the aim of covering the whole UWB frequency band, a semi-circular structure and an arc-shaped structure are formed on the radiating element, and finally to further improve the matching we have varied the length of the patch L1 from 10 to 8.3 mm as depicted in figure 3 that depicts the adaptation of the single antenna as a function of different value of L1. Figure 2 and table 1 represent respectively the design evolution of the proposed unit antenna and the optimized dimensions.

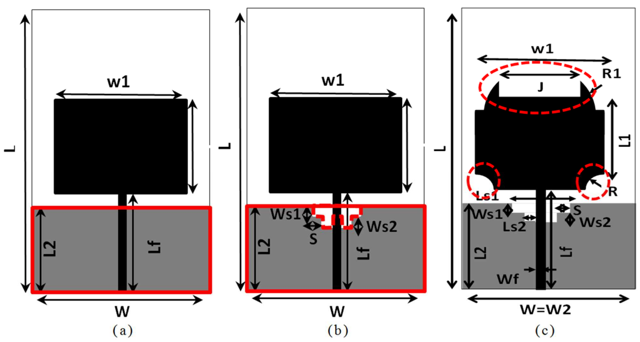


***Figure 2.*** *Design evolution of the studied monopole antenna, (a) Antenna configuration 1. (b) Antenna configuration 2. (c) Antenna configuration 3.*

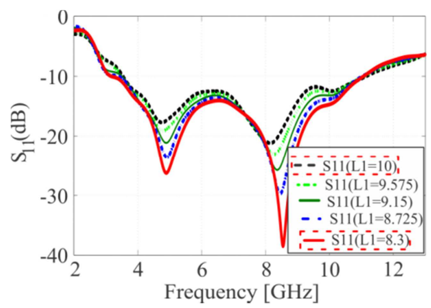


***Figure 3.*** *Reflection coefficient as a function of antenna length.*

***Table 1.*** *Dimensions of the studied UWB unit antenna in (mm).*

| | | | | | | | | |
|---|---|---|---|---|---|---|---|---|
| L | $L_1$ | $L_2$ | $L_F$ | $L_{S1}$ | $L_{S2}$ | W | $W_1$ | $W_2$ |
| 31 | 8.3 | 8 | 9 | 4 | 1 | 15.5 | 10 | 15.5 |
| $W_F$ | $W_{S1}$ | $W_{S2}$ | S | R | $R_1$ | J | T | H |
| 1 | 0.8 | 1 | 0.5 | 2.5 | 5 | 6 | 0.035 | 0.8 |

### *2.2. 2×2 MIMO Antenna*

Based on reference [10], an analysis of two designs that belong to 2×2 MIMO antenna assembly is done in this part. Noting that the radiating elements used in this study are evolved from the previous proposed single antenna element. The first design consists of two alongside arranged adjacent elements, while in the second design, the radiators are placed orthogonally to each other. Figures 4 and 5 illustrate both of 2×2 MIMO antenna designs and their comparison in terms of s-parameters. Knowing that the distance between radiators was chosen to be 0.7 λ for the first design and 0.6 λ for the second one. Results show that the polarization diversity technique that corresponds to the second design is more efficient in terms of isolation enhancement since it achieves an electromagnetic coupling less than 22 dB in comparison with space diversity technique that gives a mutual coupling of about 11.81 dB. Figure 7 and table 2 represent respectively the studied four elements UWB MIMO antenna and its dimensions.

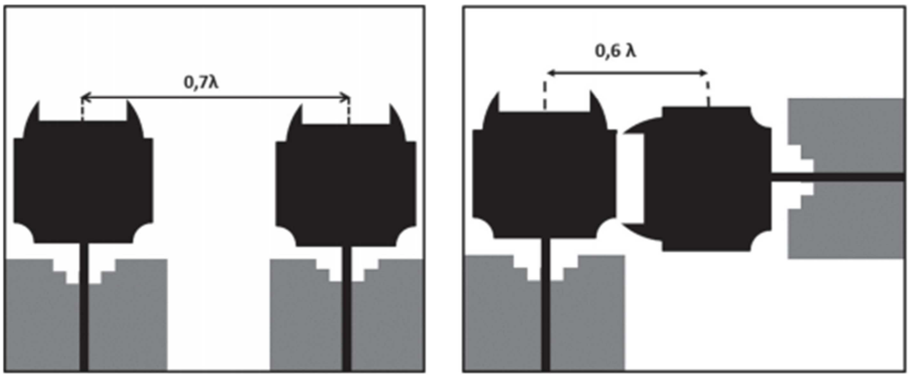


(a) (b)

***Figure 4.*** *The analyzed MIMO antenna two models, (a) first model, (b) second model.*

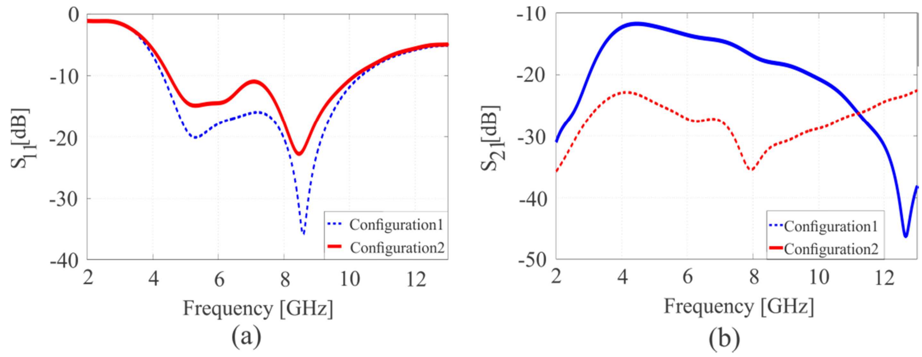


***Figure 5.*** *Simulated s-parameters of configuration 1 and 2 (a) S11, (b) S21.*

### *2.3. 4×4 MIMO Antenna Assembly*

In the same way, the study of a 4×4 MIMO antenna assembly has been done, using the single antenna element discussed in the first section. However, since the electromagnetic coupling amid antenna adjacent elements alter the impedance matching, a parametric study has been redone on radiators in order to improve adaptation. The first step of this design is to maintain a good isolation between radiators with no use of decoupling mechanism so as to achieve a compact size. To do this, we employed the polarization diversity technique since the previous study proves that this latter gives pretty good results. Despite of this step, the isolation and the impedance matching were not enhanced over all the UWB bandwidth. So as a solution, the effect of different values of L1 on isolation has been studied. It is obvious from figure 6(a) that exhibits the proposed antenna mutual coupling with varying L1, that as L1 decreases a low electromagnetic coupling has been obtained.

***Table 2.*** *The proposed 4×4 MIMO antenna optimized dimensions in (mm).*

| Parameter | Value | Parameter | Value |
|---|---|---|---|
| L | 31 | Wf | 1.5 |
| L1 | 6.8 | Wd | 1 |
| L2 | 9 | Ws1 | 1.8 |
| Lf | 9 | Ws2 | 3 |
| Ld | 1.2 | W3 | 4 |
| Ls1 | 4 | R | 4 |
| S | 1 | R1 | 5 |
| W | 31 | Rn | 2.5 |
| W1 | 10.5 | T | 0.035 |
| W2 | 11 | H | 0.8 |

Furthermore, in order to shift the lower frequency, a parametric analysis has been made too on R and J as depicted in figure 6(b), which proves that as R increases and J decreases, the lower frequency shifts from 4.3 to 3.75 GHz. Moreover, an optimization on the ground plane parameters that affect more the impedance matching has been done. Figure 6 (c) shows S11 with varying L2, Ws1, Ws2, and Wf. It is obvious that by varying L2 from 8 to 9, ws1 from 0.8 to 1.8, ws2 from 1 to 3 and $W_f$ from 1 to 1.5, a good impedance matching has been achieved.

At the end, to extend the frequency band at the lower frequency band level with the purpose of covering the UWB frequency band as well as to enhance more and more the adaptation, a DMS and DGS have been used on the feedline and on the ground plane of each antenna elements, respectively. Figure 6(d) and (e) represent the effect of both DMS and DGS on the reflection coefficient. As we can see on these figures, the utilized techniques (DMS and DGS) had a good impact on impedance matching improvement.

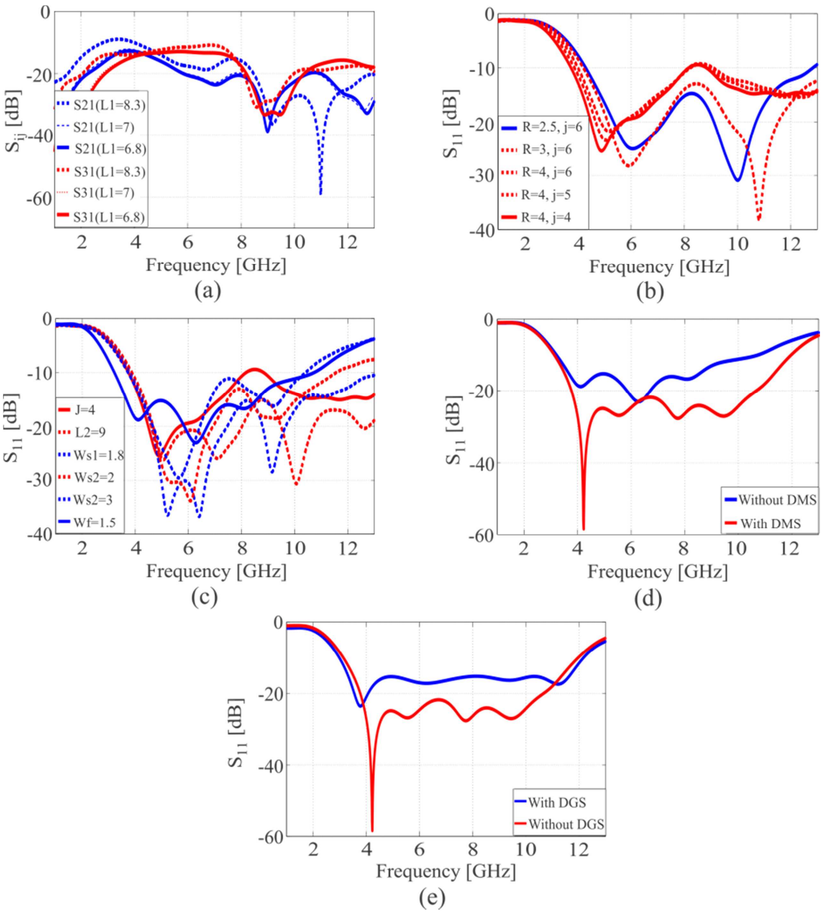


***Figure 6.*** *The optimization evolution of four-element MIMO antenna main parameters, (a) S21 and S31 with varying L1, (b) S11 with varying R and J, (c) S11 with varying L2, Ws1, Ws2, and, Wf, (d) S11 with and without DMS, (e) S11 with and without DGS.*

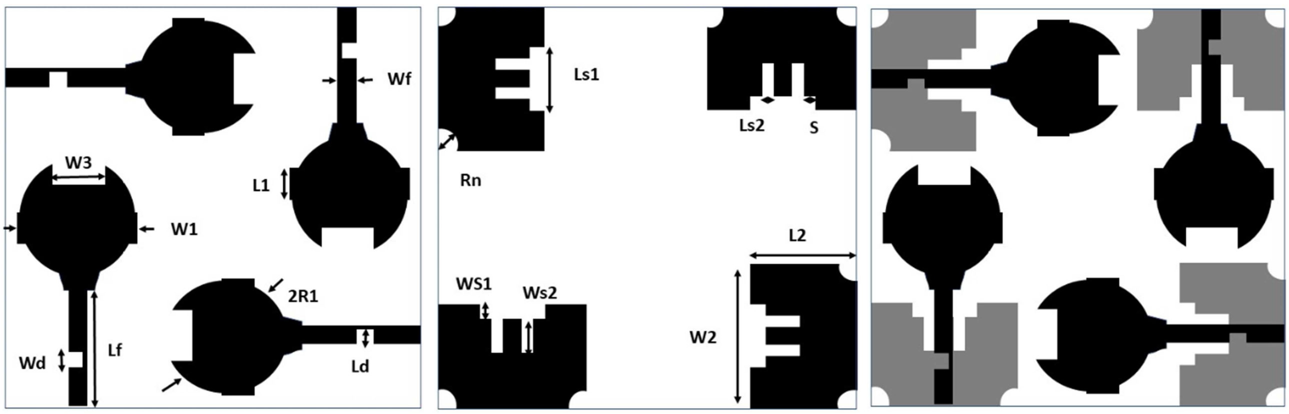


(a) (b) (c)

***Figure 7.*** *The proposed four-element MIMO antenna, (a) top face, (b) bottom face, (c) overall MIMO antenna.*

#### *2.3.1. Current Repartition*

To more analyze the impact of the chosen configuration on the inter-element mutual coupling, current repartition of the proposed UWB MIMO antenna at 5 GHz is discussed here. Figure 8 indicates the current repartition of the studied 4×4 UWB MIMO antenna. It is trivial from the depicted figure that due to the perpendicular placement of antenna elements, the surface current propagation and nearfield coupling across ports is neglected, which proves low mutual coupling among antenna elements.

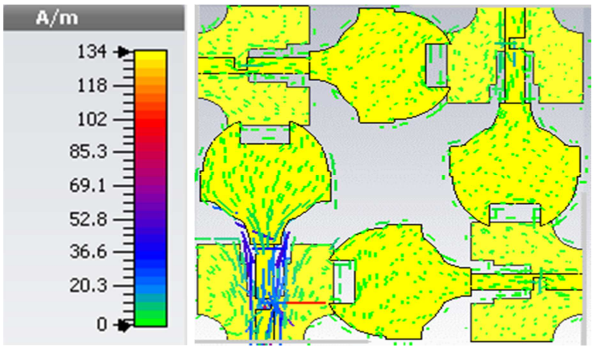


***Figure 8.*** *The UWB MIMO antenna current repartition at 5 GHz.*

#### *2.3.2. Antenna Efficiency*

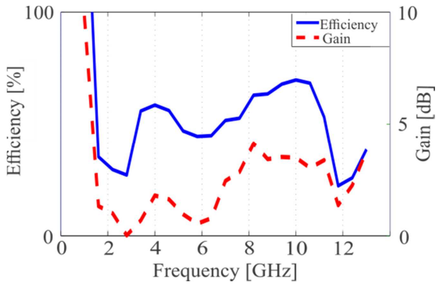


***Figure 9.*** *The proposed MIMO antenna. efficiency and gain*

The radiation efficiency is considered as a significant parameter to evaluate the loss of the antenna. In paper [11], it is defined as radiated power to input power ratio. Figure 9 shows the studied UWB MIMO antenna assembly efficiency and gain. As depicted, the presented antenna provides a high efficiency that ranges between 50% and 70% with a gain that equal 4 dBi. From these results, we can say that the employment of the FR-4 substrate does not impact the antenna efficiency.

#### *2.3.3. Impedance Matching Verification*

The ultimate step before moving to the fabrication process of the proposed antenna design is to verify the input impedance. Figure 10 represents the input impedance of the presented MIMO antenna.

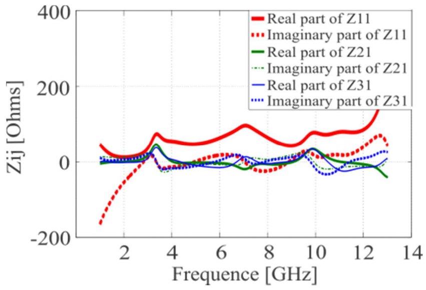


***Figure 10.*** *The input impedance of the designed MIMO antenna.*

As shown, the adaptation is well attained over the interested frequency band which makes this design ready to be fabricated.

#### *2.3.4. Fabrication Process*

For prototype fabrication, a LPKF ProMat C60 printed circuit board (PCB) plotter was used as well as a double face FR-4 substrate, see article [12] for the used substrate specifications. In addition, at the measurements level, 50 Ω SMA (Sub Miniature version A) connectors were used to excite the prototype and a Rohde&Schwarz ZVB 20 vector network analyzer (VNA) is used as well to get the proposed MIMO antenna s-parameters (see article [13,14] for more information about this VNA). The prototype of the UWB MIMO antenna is illustrated in figure 11.

The experimental results show that the presented 4×4 UWB MIMO antenna gives a -10 dB impedance bandwidth that ranges from 3 to 12.8 GHz and a high isolation more than 15 dB. Figure 12 represents measured and simulated S-parameters comparison. Noting that the discrepancy between the experimental and the simulated results is due to many factors which are fabrication imprecision, ports connections, and soldering.

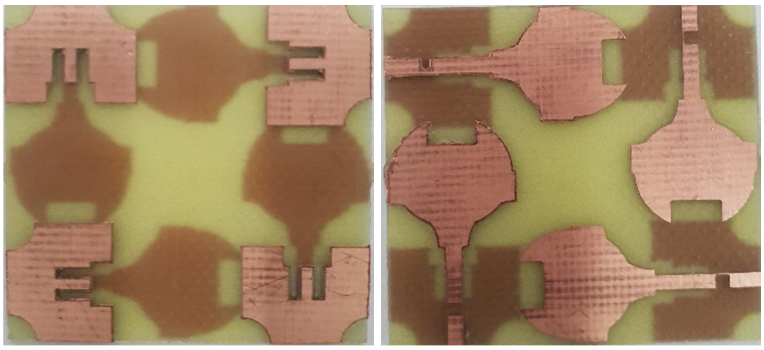

***Figure 11.*** *The studied four elements MIMO antenna prototype.*

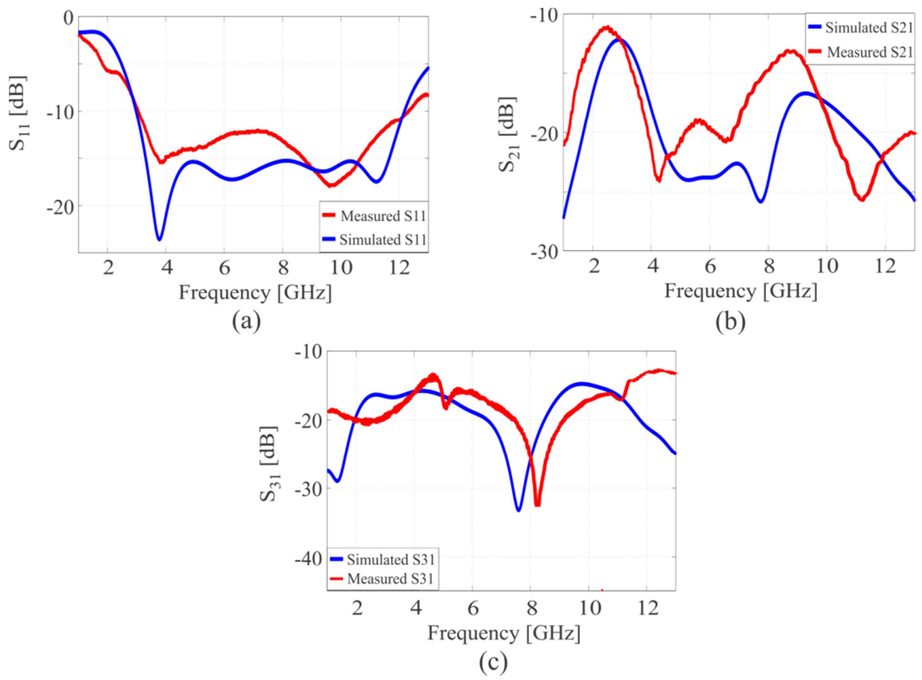


***Figure 12.*** *The measured and simulated S-parameters, (a) S11, (b) S21, (c) S31.*

# 3. Evaluation of Antenna Performance

## *3.1. Correlation Coefficient*

The correlation of a certain antenna array defines the degree of independence of the individual antenna elements. This parameter $\boldsymbol{\rho_e}$is defined in the research [15] by this following formula:

$$\rho_e \approx \left( \frac{\oint \left( XPR.E_{\theta X} E^*_{\theta Y} P_\theta + E_{\phi X} E^*_{\phi Y} P_\phi \right) d\Omega}{\sqrt{\oint \left( XPR.E_{\theta X} E^*_{\theta X} P_\theta + E_{\phi X} E^*_{\phi X} P_\phi \right) d\Omega \oint \left( XPR.E_{\theta Y} E^*_{\theta Y} P_\theta + E_{\phi Y} E^*_{\phi Y} P_\phi \right) d\Omega}} \right)^2 \quad (5)$$

Where $E_{\theta,\phi X}$ et $E_{\theta,\phi Y}$ are the electric field patterns that correspond to antennas X and Y, respectively in the antenna assembly. The threshold for getting high performance is $\rho_e$ <0.5. Noting that In a MAS (Multiple Antenna Systems), this degree of independence can be altered by the distance between radiating elements, antenna directivity, ground plane, Q factors,...etc.

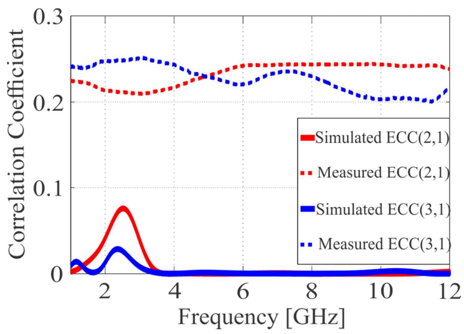


***Figure 13.*** *The measured and simulated correlation coefficient.*

Figure 13 shows the studied antenna simulated and measured correlation coefficient comparison. it is trivial that the studied antenna gives a low ECC less than <0.3 over all the UWB frequency band.

## *3.2. Diversity Gain*

Compared to the SNR received from a unit antenna, the combined SNR improvement of the Multiple Antenna Systems is defined as the Diversity Gain (DG). This latter is given in research [16] as:

$$\mathrm{DG} = \left. \frac{\left(\frac{r_C}{\Gamma_C}\right)}{\left(\frac{r}{\Gamma}\right)_{\text{Best branch}}} \right|_{P_{r_C}} \quad (6)$$

where $r$ and et $r_C$ are instantaneous SNRs, $\Gamma$ and $\Gamma_C$ are average SNRs for the combined and best single antenna branch signals, respectively. And $P_{r_C}$ is the probability.

Noting that taking into account the total efficiency degradation when talking about multiple antenna systems, the effective diversity gain (EDG) becomes more useful than diversity gain parameter since it takes into consideration the antenna total efficiency as exposed in [17].

$$\mathrm{EDG} = \left. \frac{\left(\frac{r_C}{\Gamma_C}\right)}{\left(\frac{r}{\Gamma}\right)_{\text{Best branch}}} \right|_{P_{r_C}} \cdot \eta_{\text{Best branch}} \quad (7)$$

Where the best branch η is the total efficiency.

As explained in article [18], with the aim to verify whether it is advantageous to utilize an antenna assembly or a single antenna in a certain small device, the actual diversity gain (ADG) is defined.

$$DG = \left.\frac{\left(\frac{r_C}{\Gamma_C}\right)}{\left(\frac{r}{\Gamma}\right)_{\text{single antenna solution}}}\right|_{P_{r_C}} \quad (8)$$

As we can observe from figure 14 that depicts the presented antenna diversity gain, it is clear that DG21 and DG31 equal to 8.75 which verify furthermore the studied antenna high diversity performance.

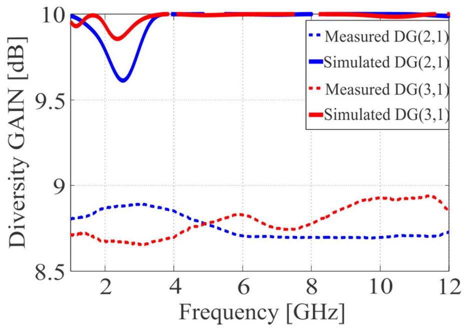


***Figure 14.*** *The diversity gain.*

### *3.3. Total Active Reflection Coefficient*

The dispersion matrix is an essential parameter that gives an idea about a certain antenna bandwidth. However, it is not quite important when we deal with a multiple antenna system, that is why a new parameter has seen the light. This parameter is called the total active reflection coefficient (TARC), and is defined in paper [19] as:

$$\Gamma_a^t = \sqrt{\frac{P_{in} - P_{rad}}{P_{in}}} \quad (9)$$

Where: $(P_{in})$ is the incident power, $(P_{rad})$ is the transferred power, and $(P_{réf})$ is the reflected power.

For a no lossy multiple antenna system, the total active reflection coefficient can be given as follows:

$$\Gamma_a^t = \frac{\sum_{i=1}^{N} |b_i^2|}{\sum_{i=1}^{N} |a_i^2|} \quad (10)$$

Where $b_i$ and $a_i$ are the incident and reflected signal vectors with random phase elements, respectively.

According to four-element MIMO antenna assembly, as shown in reference [20] formula (10) could be written as follow:

$$\begin{bmatrix} b1 \\ b2 \\ b3 \\ b4 \end{bmatrix} = \begin{bmatrix} S11 & S12 & S13 & S14 \\ S21 & S22 & S23 & S24 \\ S31 & S32 & S33 & S34 \\ S41 & S42 & S43 & S44 \end{bmatrix} \begin{bmatrix} a1 \\ a2 \\ a3 \\ a4 \end{bmatrix} \quad (11)$$

Figure 15 exhibits the measured total active reflection coefficient, as we can see from this figure, the measured TARC is less than -10 dB over all the UWB frequency band, which proves the good impedance matching of the whole antenna system.

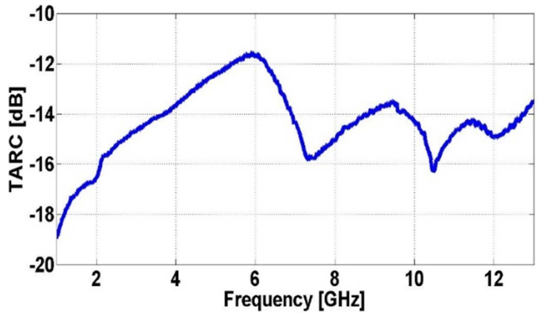


***Figure 15.*** *The measured Total Active Reflection Coefficient.*

### *3.4. Farfield Pattern*

The kit (antenna measurement systems from Geozondas) we used for farfield pattern measurements is based on pulse (time domain), see reference [21]. As presented in the below 2D radiation patterns representation, it is obvious that the antenna prototype provides a good radiation behavior that agree well with the simulated one. Figure 16 represents the simulated and measured farfield patterns at 4, 6 and 8 GHz for E plane and H plane.

### *3.5. Capacity Loss*

Generally, the increase of the MIMO antenna radiating elements results an improvement at the channel capacity level. However, uncorrelated Rayleigh fading induces a channel capacity loss (CCL) of the overall multiple anntenna system. This channel capacity loss (Closs) can be calculated based on the following formula that is extracted from paper [22]:

$$C_{loss} = -log_2 det(\psi^R) \quad (12)$$

Where $\psi^R$ is the correlation matrix of the receiving antenna which is expressed by:

$$\psi^R = \begin{bmatrix} \rho_{1j} & \cdots & \rho_{1N} \\ \vdots & \ddots & \vdots \\ \rho_{N1} & \cdots & \rho_{Nj} \end{bmatrix} \quad (13)$$

$$\rho_{ii} = 1 - |\sum_{n=1}^{N} S_{in}^* S_{ni}|, \rho_{ij} = -\left|\sum_{n=1}^{N} S_{in}^* S_{nj}\right|, pour\ i,j = 1,2,3,\dots ou\ N. \quad (14)$$

The evaluated channel capacity loss that corresponds to the studied MIMO antenna is shown in figure 17. From this latter, it is trivial that the measured channel capacity loss that corresponds to this antenna is lower than 0.05 bits/s/Hz over the whole frequency band of interest, which proves that having low electromagnetic coupling and high efficiency will result a neglected channel capacity loss.

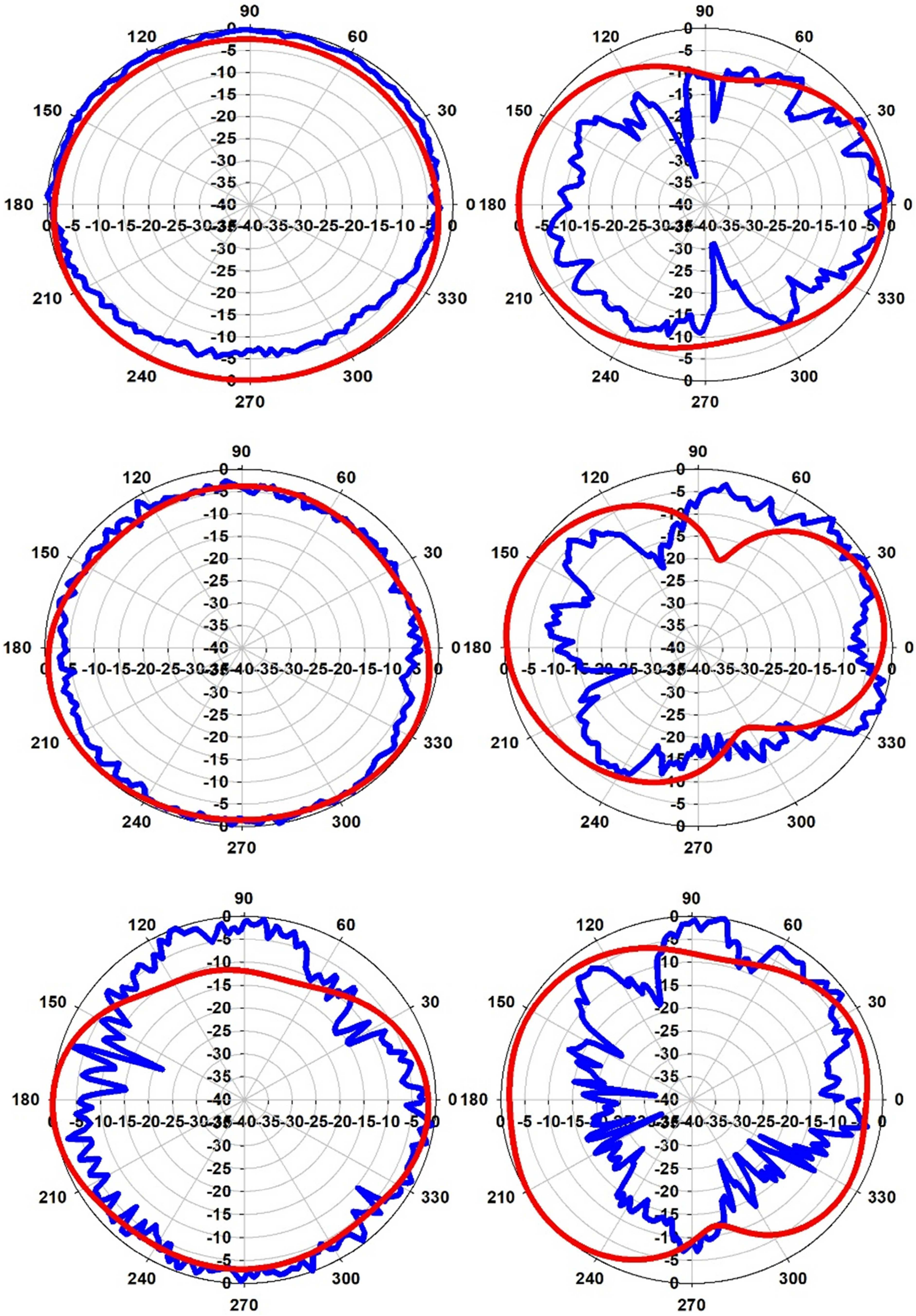


(a) (b)

***Figure 16.*** *Radiation pattern of the analyzed MIMO antenna, (a) E-plane, (b) H-plane.*

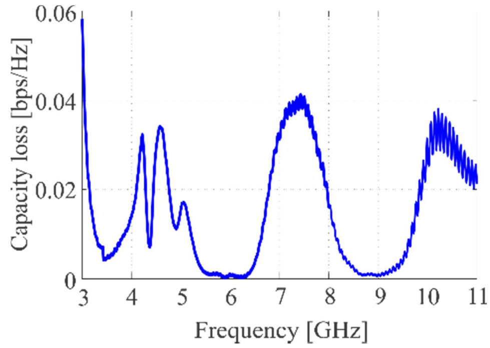


***Figure 17.*** *Measured total capacity loss of the proposed MIMO antenna.*

# 4. Comparison

To evaluate the utility of this work, the diversity performance parameters of the presented 4×4 MIMO antenna and works from literature are compared. Table 3 exhibits this comparison.

The presented MIMO assembly is proposed for UWB applications. Literature describes many UWB MIMO antenna system. Although, the studied design is a potential one compared to the recently reported ones, especially in terms of size. The analyzed UWB MIMO antenna specifications comparison with reported works is depicted in table 3. As this table show, the analyzed UWB MIMO antenna exhibits not only a miniaturized size but also provides a good diversity performance, which enable us to say that it is considered as a good candidate for UWB applications.

***Table 3.*** *Antenna specifications comparison with reported researches.*

| Ref | Size (mm) | Bandwidth (GHz) | Isolation (dB) | ECC |
|---|---|---|---|---|
| [23] | 60*60 | 2.73-10.68 | <-15 | <-28 |
| [24] | 110*60 | 2.2-2.5 | <-11 | <0.3 |
| | | 2.4-2.5 | | |
| [25] | 35*38 | 3.4-3.6 | <-16 | <0.05 |
| | | 5-5.5 | | |
| This work | 31*31 | 3-12.18 | <-15 | <0.3 |

# 5. Conclusion

In this work, a novel minimized-coupling MIMO antenna assembly has been proposed for high data rate UWB applications. The overall antenna system is constituted by four radiating elements. In order to get a high isolation among adjacent elements and maintain the antenna compactness, the polarization diversity technique is used in combination with miniaturization techniques. Using these techniques, the electromagnetic coupling has been minimized significantly as well as a compact dimension of the proposed MIMO antenna assembly has been realized. It has been shown that measured results agree well with simulated ones, either in terms of radiation performances or diversity antenna ones. Results indicate that miniaturization mechanisms can be considered as one of the essential techniques which can help us to develop compact antenna array without using decoupling techniques so as to prevent bulky antenna systems, especially when it comes to UWB applications.

# Data Availability Statement

All data generated during this study are included in this published article.

# Conflict of Interests

The authors declare that there is no conflict of interests regarding the publication of this paper.

# Acknowledgements

This research was partially supported by National School of Applied Sciences, under sciences and advanced technologies laboratory, Abdelmalek Essaadi University, Tetuan, Morocco.

# References


[1] Haque, Sk & Alam, Hashibul. (2019). Further slot antenna miniaturization and bandwidth enhancement. International Journal of RF and Microwave Computer-Aided Engineering. 1-8. 10.1002/mmce.21732.

[2] Bhattacharjee, Anindita & Karmakar, Anirban & Saha, Anuradha & Bhattacharya, Diptendu. (2021). Design of a compact UWB MIMO ‐ diversity antenna incorporating fractal inspired isolation structure with band notch characteristics. Microwave and Optical Technology Letters. 63. 10.1002/mop.32927.

[3] Bellary, Anudeep & Kandasamy, Krishnamoorthy. K & Rao, Patnam. (2020). Mitigation of mutual coupling in 2 X 2 dual slant polarized MIMO antennas using periodic array of SRRs loaded with transmission line for LTE band 40. International Journal of RF and Microwave Computer-Aided Engineering. 30. 10.1002/mmce.22454.

[4] I. Nadeem and D. Choi, "Study on Mutual Coupling Reduction Technique for MIMO Antennas," in *IEEE Access*, vol. 7, pp. 563-586, 2019, doi: 10.1109/ACCESS.2018.2885558.

[5] S. Bukkawar and V. Ahmed, "Study of Various Mutual Coupling Reduction Techniques in MIMO Antennas," *2019 Third International Conference on Inventive Systems and Control (ICISC)*, 2019, pp. 106-113, doi: 10.1109/ICISC44355.2019.9036446.

[6] U. Sharma and G. Srivastava, "A Study of Various Techniques to Reduce Mutual Coupling in MIMO Antennas," *2020 Second International Conference on Inventive Research in Computing Applications (ICIRCA)*, 2020, pp. 1-7, doi: 10.1109/ICIRCA48905.2020.9182992.

[7] H. Werfelli, K. Tayari, M. Chaoui, M. Lahiani and H. Ghariani, "Design of rectangular microstrip patch antenna," 2016 2nd International Conference on Advanced Technologies for Signal and Image Processing (ATSIP), 2016, pp. 798-803, doi: 10.1109/ATSIP.2016.7523197.

[8] Jadaun, Veerendra & Sharma, Pavan. (2018). Design a Microstrip Patch Antenna of Singal Band for 1.8GHz.

[9] Waqas, Muhammad & Bashir, Shahid & Khan, Muhammad. (2015). High Gain Microstrip Patch Antenna using Double Negative Metamaterial. 10.1109/ICET.2015.7389171.

[10] Mchbal A, Touhami NA, Elftouh H, Moubadir M, Dkiouak A. Spatial and Polarization Diversity Performance Analysis of a Compact MIMO Antenna. Procedia Manuf 2019; 32: 647–52.

[11] Xu, Qian & Xing, Lei & Zhao, Yongjiu & Jia, Tianyuan & Huang, Yi. (2021). Probability distributions of three - antenna efficiency measurement in a reverberation chamber. IET Microwaves, Antennas & Propagation. 15. 10.1049/mia2.12155.

[12] Sanapala, Ravikumar. (2008). Characterization of FR-4 Printed Circuit Board Laminates Before and After Exposure to Lead-free Soldering Conditions.

[13] M. Magerl, T. Mandic and A. Baric, "Broadband characterization of SMA connectors by measurements," *2014 37th International Convention on Information and Communication Technology, Electronics and Microelectronics (MIPRO)*, 2014, pp. 104-109, doi: 10.1109/MIPRO.2014.6859542.

[14] Rohde & schwarz, "R & S ® Znb Vector Network Analyzer," Benjamin Franklin Drive, Columbia, USA, 2022.

[15] Imaculate Rosaline, Arvind Kumar, Prashant Upadhyay, Abu Hena Murshed, "Four Element MIMO Antenna Systems with Decoupling Lines for High-Speed 5G Wireless Data Communication", International Journal of Antennas and Propagation, vol. 2022, Article ID 9078929, 13 pages, 2022. https://doi.org/10.1155/2022/9078929.

[16] Ying Z., Chiu CY., Zhao K., Zhang S., He S. (2016) Antenna Design for Diversity and MIMO Application. In: Chen Z., Liu D., Nakano H., Qing X., Zwick T. (eds) Handbook of Antenna Technologies. Springer, Singapore. https://doi.org/10.1007/978-981-4560-44-3_53.

[17] Papamichael, Vasilis & Karadimas, Petros. (2015). New Intuitive Metrics for Diversity Performance Evaluation of Multi-element Antenna Systems.

[18] Plicanic, Vanja & Lau, Buon & Derneryd, A. & Ying, Zhinong. (2009). Actual Diversity Performance of a Multiband Diversity Antenna With Hand and Head Effects. Antennas and Propagation, IEEE Transactions on. 57. 1547 - 1556. 10.1109/TAP.2009.2016707.

[19] Chae, Sung & Oh, Se-keun & Park, Seong-Ook. (2007). Analysis of mutual coupling, correlations, and TARC in WiBro MIMO array antenna. Antennas and Wireless Propagation Letters, IEEE. 6. 122 - 125. 10.1109/LAWP.2007.893109.

[20] Elix Urimubenshi, Dominic B. O. Konditi, Jean de Dieu Iyakaremye, Pierre Moukala Mpele, Augustin Munyaneza, "A novel approach for low mutual coupling and ultra-compact Two Port MIMO antenna development for UWB wireless application", Heliyon, Volume 8, Issue 3, 2022.

[21] GEOZONDAS, "UWB antennas, sampling oscilloscopes, programmable delay lines, pulse splitters for UWB radar applications and measurement systems," 2010.

[22] M. S. Aw, K. Ashwath, P. Ramaswamy, T. Ali, and J. Anguera, "A Uniquely Shaped MIMO Antenna on FR4 Material to Enhance Isolation and Bandwidth for Wireless Applications," AEUE - Int. J. Electron. Commun., p. 153316, 2020.

[23] Nguyen Khac Kiem, Huynh Nguyen Bao Phuong, Dao Ngoc Chien, "Design of Compact 4 × 4 UWB-MIMO Antenna with WLAN Band Rejection", International Journal of Antennas and Propagation, vol. 2014, Article ID 539094, 11 pages, 2014. https://doi.org/10.1155/2014/539094

[24] Hassan, A. T., Sharawi, M. S. Four element half circle shape printed MIMO antenna. Microw Opt Technol Lett 2016; 58: 2990-92. doi: 10.1002/mop.30201.

[25] Karimian R, Soleimani M, Hashemi SM. Tri-band four elements MIMO antenna system for WLAN and WiMAX application. J Electromagn Waves Appl 2012; 26: 2348–57. doi: 10.1080/09205071.2012.734433.